MEASUREMENTS OF DIRECT CP VIOLATION IN THE NEUTRAL KAON SYSTEM

Alexandre Glazov
Enrico Fermi Institute
University of Chicago, Chicago, IL 60637

Representing the KTeV Collaboration

ABSTRACT

This paper presents new measurements of direct CP violation in the neutral kaon system performed by the two fixed target experiments, NA48 at CERN and KTeV at Fermilab. The data establishes a non-zero value of $\mathrm{Re}(\epsilon'/\epsilon) = (19.3 \pm 2.4) \times 10^{-4}$ (world average). The result is consistent with the Standard Model expectations and rules out Superweak models as the sole source of the CP violation in the neutral kaon system.

The emphasis of this paper is on experimental techniques which made this measurement possible. We describe the KTeV experiment in somewhat more detail than NA48. Similarities and differences between the two detectors are highlighted.

1 Introduction

Since the discovery of the K^0, $\overline{K^0}$ mixing in the 1950s, the system of neutral kaons has attracted the attention of physicists as an outstanding laboratory for precision study of extremely small effects. The observable states, K_L and K_S, have a tiny mass splitting (Δm) but a large lifetime difference. The latter allows the clean separation of K_L particles which led in 1964 to the discovery of the CP violating decay $K_L \to \pi\pi$.[1]

The gross features of the CP violation in the neutral kaon system are due to CP asymmetric mixing or *indirect* CP violation. The CP eigenstates for K^0, $\overline{K^0}$ particles are CP even and CP odd states, K_1 and K_2:

$$\begin{aligned} K_1 &\sim K^0 + \overline{K^0}\,, \\ K_2 &\sim K^0 - \overline{K^0}\,. \end{aligned} \tag{1}$$

If the neutral kaons obeyed CP symmetry, the K_S and K_L particles would coincide with K_1 and K_2, respectively. This actually explains the lifetime difference: K_S is allowed by CP to decay into the $\pi\pi$ state which has a much larger phase space compared to all the CP-allowed K_L decays. Yet the presence of the $K_L \to \pi\pi$ decay means that K_L contains some CP even admixture:

$$\begin{aligned} K_S &\sim K_1 + \epsilon K_2\,, \\ K_L &\sim K_2 + \epsilon K_1\,. \end{aligned} \tag{2}$$

The smallness of CP violation is expressed by the smallness of the CP violating mixing parameter, $2\mathrm{Re}(\epsilon) = 0.00327 \pm 0.00012$.[2]

The other possible source of CP violation comes from the decay process by itself and is usually referred as *direct* CP violation. Assuming CPT conservation, the decay amplitudes into final states with different isospin I are written

$$\begin{aligned} \langle I|T|K^0\rangle &= A_I e^{i\delta_I}\,, \\ \left\langle I|T|\overline{K^0}\right\rangle &= A_I^* e^{i\delta_I}\,, \end{aligned} \tag{3}$$

where $I = 0, 2$ and δ_I are final state interaction phase shifts. We can write the ratio of K_L to K_S decay amplitudes into the two 2π final states, $\pi^+\pi^-$ ("charged mode") and $\pi^0\pi^0$ ("neutral mode"), as

$$\begin{aligned} \eta_{+-} &= \epsilon + \epsilon', \\ \eta_{00} &= \epsilon - 2\epsilon'. \end{aligned} \tag{4}$$

Here ϵ' is given by

$$\epsilon' = \frac{i}{\sqrt{2}} e^{i(\delta_2 - \delta_0)} \frac{\mathrm{Re}(A_2)}{\mathrm{Re}(A_0)} \left(\frac{\mathrm{Im}(A_2)}{\mathrm{Re}(A_2)} - \frac{\mathrm{Im}(A_0)}{\mathrm{Re}(A_0)} \right). \tag{5}$$

The phase of ϵ is determined by the K_L-K_S mass difference, Δm, and the lifetime difference. It is about $\phi_\epsilon = 43.5°$. The phase of ϵ', $\phi_{\epsilon'} = \pi/2 + \delta_2 - \delta_0 = 48 \pm 4°$, according to the measurement of the final state phase shifts.[3] Therefore, in the absence of CPT violation, the ϵ and ϵ' vectors are nearly parallel and using equation (4) we can write:

$$\mathrm{Re}(\epsilon'/\epsilon) = \frac{1}{6}\left(1 - \left|\frac{\eta_{00}}{\eta_{+-}}\right|^2\right) = \frac{1}{6}\left(1 - \frac{\dfrac{\Gamma(K_L \to \pi^0\pi^0)}{\Gamma(K_S \to \pi^0\pi^0)}}{\dfrac{\Gamma(K_L \to \pi^+\pi^-)}{\Gamma(K_S \to \pi^+\pi^-)}}\right). \tag{6}$$

In the Standard Model, the kaon mixing is explained by a box diagram with virtual W exchange. This indirect CP violation is naturally accommodated by the complex phase in the CKM quark mixing matrix. The Standard Model *predicts* existence of the direct CP violation, although exact calculations are difficult and under some circumstances $\mathrm{Re}(\epsilon'/\epsilon)$ may vanish since the dominant diagrams have contributions of the opposite sign. Recent calculations estimate $\mathrm{Re}(\epsilon'/\epsilon)$ between 5×10^{-4} and 30×10^{-4}.

Alternatively, CP violation can be described by the Superweak model,[4] which introduces an additional CP violating interaction, analogously to the standard weak interaction which violates parity. The Superweak model has no direct CP violation, $\mathrm{Re}(\epsilon'/\epsilon)_{SW} = 0$. Therefore, measuring a non-zero value of $\mathrm{Re}(\epsilon'/\epsilon)$ confirms the Standard Model and rules out the Superweak model as a sole source of the CP violation.

In the 1980's and early 1990's two groups, at CERN and at Fermilab, undertook experiments to measure $\mathrm{Re}(\epsilon'/\epsilon)$. The results obtained by NA31 at CERN, $\mathrm{Re}(\epsilon'/\epsilon) = (23. \pm 6.5) \times 10^{-4}$, and by E731 at Fermilab, $\mathrm{Re}(\epsilon'/\epsilon) = (7.4 \pm 5.2) \times 10^{-4}$, are in fair agreement although they carry different messages: the CERN result establishes direct CP violation at about 3.5σ level while the Fermilab result is consistent with $\mathrm{Re}(\epsilon'/\epsilon) = 0$. The average of the experiments, $\mathrm{Re}(\epsilon'/\epsilon) = (15 \pm 8) \times 10^{-4}$, establishes the effect at the 2σ level only. Both groups decided to perform new experiments with a design precision of a few $\times 10^{-4}$ to clarify the matter. The new experiments are KTeV at Fermilab and NA48 at CERN.

The measurement of $\mathrm{Re}(\epsilon'/\epsilon)$ at a sub-per-mil level using formula (6) is challenging. First of all, high intensity kaon beams are needed to detect several million CP violating $K_L \to \pi^0\pi^0$ decays. The double ratio form of equation (6) suggests cancellation of systematic uncertainties, which are common for the decays into the same final state and also for decays of the same particles into different final states. Yet, in general the cancellation is not perfect and requires careful detector design as well as scrupulous data analysis.

The next section describes the design and basis of the data analysis at the two experiments. We will try to emphasize similarities and alternative paths used by the collaborations. The paper is based on the first $\mathrm{Re}(\epsilon'/\epsilon)$ measurements by the collaborations. These are the KTeV measurement based on 1996 data and the first part of the 1997 data,[5] the NA48 measurement is based on 1997 data,[6] and the NA48 preliminary result is based on 1998 data.[7] The paper also uses some results based on the complete set of 1997 KTeV data, although this analysis has not been finalized in terms of the new measurement of $\mathrm{Re}(\epsilon'/\epsilon)$ yet.

2 Experiments to measure direct CP violation

Both the CERN and Fermilab experiments are fixed target detectors using secondary high energy neutral beams. The kaon energy range is $40 - 160$ GeV for KTeV and $70 - 170$ GeV for NA48. Both detectors are situated about 100 m downstream from the primary target to obtain beams of K_L, neutrons and neutral hyperons with small contamination of K_S. The primary targeting angle and additional beryllium absorbers are used to optimize the kaon to baryon flux ratio.

The key feature for both experiments is the so-called *double beam* technique: decays of K_S and K_L are detected simultaneously, for both the charged and neutral mode. The primary particle is determined using the horizontal decay vertex position (KTeV) or from the timing tagging (NA48). The experiments differ in the way the K_S particles are produced. KTeV uses two parallel K_L beams, one of which has a fully active plastic *Regenerator*, situated close to the decay volume, to produce K_S in a coherent regeneration process. NA48 has a secondary K_S production target. Some of the primary protons are transported to this target; they are detected by an array of scintillator counters to provide timing tagging.

Both experiments have similar setups to detect two track $K \to \pi^+\pi^-$ and four gamma $K \to \pi^0\pi^0$ events. The tracking consists of two stations of drift chambers, before and after an analysis magnet. The calorimetry of the experiments is superb. KTeV uses an array of CsI crystals while NA48 has chosen a quasi-homogeneous liquid krypton calorimeter. Both devices have excellent resolution; they are calibrated to a sub-per-mil level using electrons from numerous semileptonic $K_L \to \pi e \nu$ ($Ke3$) decays.

The next two subsections describe the two experiments in more detail.

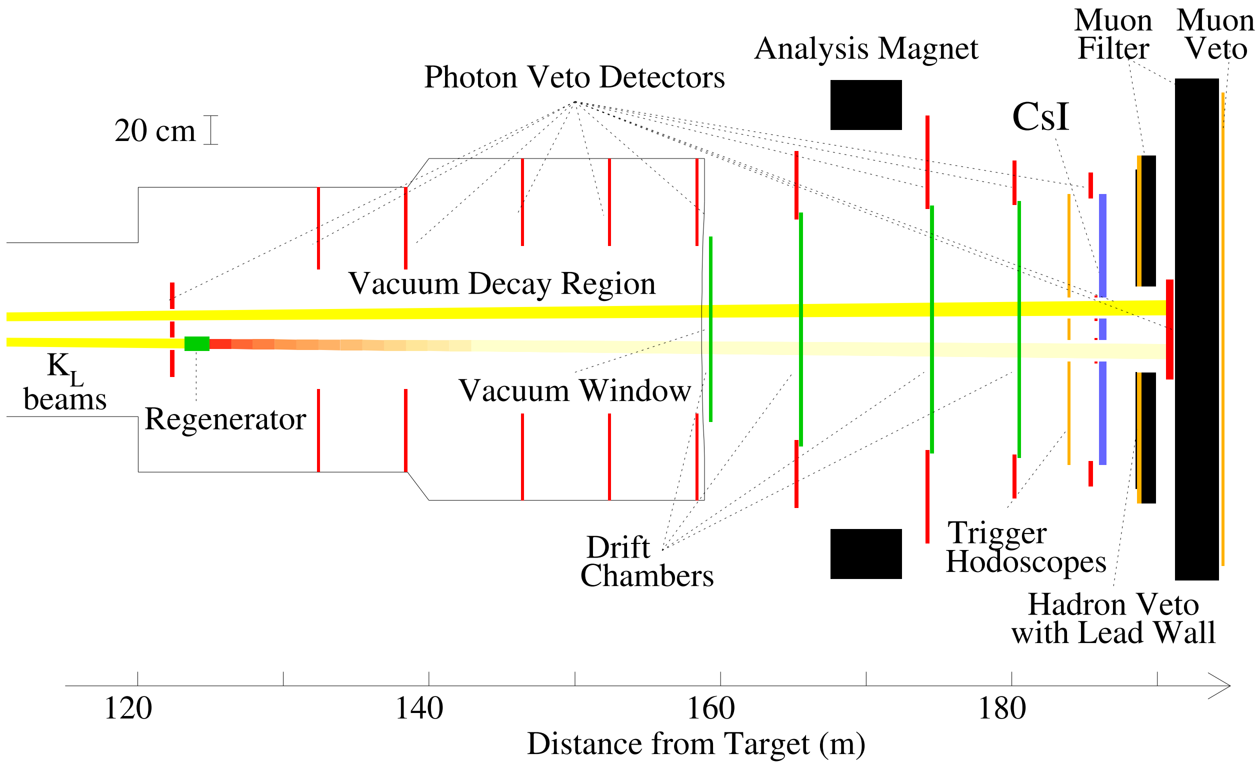

Fig. 1. The KTeV detector configuration used for the Re(ϵ'/ϵ) measurement.

2.1 The KTeV detector

A diagram of the KTeV detector is shown in Figure 1. The kaon beams are produced by an 800 GeV primary proton beam striking a BeO target. About half of $(2-8)\times 10^{12}$ protons per spill interact with the target. A set of sweeping magnets removes a large fraction of the charged particles, reducing the flux of muons reaching the detector to below 100 KHz. A set of collimators produces two identical beams that diverge by ± 0.8 mrad in the horizontal view. Beryllium and lead absorbers are placed into the beams to improve the kaon to neutron flux ratio.

Two identical kaon beams enter the fiducial volume of the detector at about 110 meters downstream from the primary target. The vacuum decay region is from about 110 to 159 meters. The decay volume is surrounded by a set of photon veto detectors to suppress neutral mode background originating from $K_L \to 3\pi^0$ events with missing photons. Inside the decay volume, the beams are separated by about 10 cm in the horizontal (X) view.

At about 125 meters from the primary target, one of the K_L beams passes through about 1.7 meters of plastic scintillator *Regenerator*. We will name this beam *Regenerator* as opposed to the other *Vacuum* beam. Since K^0 and $\overline{K^0}$ particles have different interaction cross sections with ordinary matter, the kaon beam downstream of Regenerator contains some admixture of K_S. The large decay width of the $K_S \to \pi\pi$ process means that K_S decays are dominant in the Regenerator beam. In fact, to balance the rate of $K_{S,L} \to \pi\pi$ decays and also to improve the kaon to neutron flux ratio, an additional beryllium absorber is placed upstream in the Regenerator beam. The total transmission of the Regenerator beam is about 8%; the regeneration amplitude ρ at a kaon energy of 70 GeV is about 1.2%

Once per minute the Regenerator and the additional beryllium absorber are moved from one beam to another, providing identical experimental conditions for collecting decays of K_S and K_L particles.

The length of the Regenerator is optimized to enhance *coherent regeneration* – regeneration without transverse momentum transfer, $P_t^2 = 0$, coherently summed over interactions throughout the Regenerator material. To veto inelastic interactions, the Regenerator is made of blocks of scintillators viewed by photomultiplier tubes providing veto signals at the trigger level. The remaining type of non-zero p_t^2 regeneration, originating from diffractive scattering, is studied in detail for $\pi^+\pi^-$ events, for which a measurement of p_t^2 is possible, modeled and subtracted as a background (see section 3).

The signal from the plastic scintillator is also used to veto $\pi^-\pi^+$ decays occurring inside the Regenerator. The last 2 cm long module of the Regenerator consists of two 0.56 cm lead plates sandwiched with 0.44 cm scintillator plates. This provides eight radiation lengths for four photons (2 radiation lengths for each photon) from $\pi^0\pi^0$ events and defines the sharp boundary of the decay region for the neutral mode.

At 159 meters the kaon decay products leave the vacuum decay volume through a 0.58 mm thick Kevlar window and enter the active detector which consists of drift chambers, analysis magnet, scintillator trigger hodoscope, CsI electromagnetic calorimeter and a set of hadron and muon veto detectors.

The charged particle spectrometer comprises four stations of drift chambers, two before and two after the analysis magnet. Each station contains four planes of drift chambers, two with wires in the horizontal and two with wires in the vertical direction, to measure drift distances in the vertical (Y) and horizontal (X) plane, respectively. To minimize multiple scattering, the space between the drift chambers is filled with helium contained in plastic bags at atmospheric pressure. The analysis magnet provides a horizontal momentum kick of 0.412 GeV/c.

The KTeV electromagnetic calorimeter is a square array consisting of 3100 blocks of cesium iodide crystals. Two sizes of blocks were used: 2.5×2.5 cm in the central region and 5×5 cm on the outside. All blocks are 50 cm long, which corresponds to 27 radiation lengths. The scintillation light from each CsI block is collected by a photomultiplier tube.

The channel gains are calibrated using electrons from $K_L \to \pi e \nu$ decays. For the 1996 running period, a total of 1.9×10^8 electrons was collected during the nominal running. This amount was nearly doubled for the 1997 data, allowing detailed studies of the block by block energy linearity. The results of this calibration are presented in Figure 2. The average energy resolution is below 0.7%, a value which is superior to all large detectors used in high energy physics.

2.2 The NA48 detector[6]

The NA48 detector has two separate production targets for K_L and K_S particles, located 126 m and 6 m upstream of the beginning of the decay region. For each SPS pulse, 1.1×10^{12} protons hit the K_L production target. Some of the non-interacting primary protons impinge on a bent silicon mono-crystal. A small fraction of these protons undergo channeling, and are bent to produce a collimated beam of 3×10^7 protons per

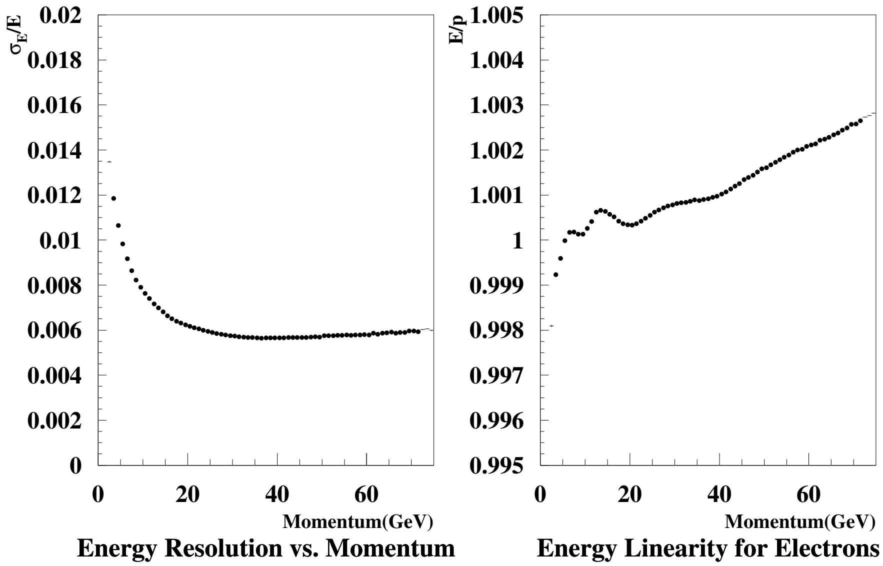

Fig. 2. Results of the KTeV CsI calibration with electrons for the 1997 run period. The left plot represents the measured calorimeter resolution as a function of electron momentum. The right plot shows the linearity of the CsI response.

pulse transported to the K_S production target. The production angles of K_L and K_S are optimized to minimize the difference in momentum spectra. The K_S beam enters the decay volume 68 mm above (Y view) the K_L beam. The beams converge at 0.6 mrad angle such that the axes of the two beams cross at the position of the electromagnetic calorimeter.

The protons directed to the K_S target are detected by an array of scintillator counters. This device is used to tag K_S decays. The presence (absence) of a proton detected in coincidence with the event defines the event as K_S (K_L). The proton time resolution is 120 ps and the double-pulse separation is 4 ns.

The neutral beam produced at the K_S target traverses an anti-counter, formed by a set of three scintillator counters preceded by an aligned 3 mm thick iridium crystal which enhances photon conversion (1.8 effective radiation lengths). This detector is used for an accurate definition of the beginning of the decay region.

The decay volume is contained in an evacuated 90 meter long tank surrounded by photon veto counters. The decay particles enter the detection volume through a 0.9 mm thick Kevlar window; the neutral beam continues in a 16 cm evacuated beam pipe.

The active volume of the NA48 detector has the same components as KTeV. The magnetic spectrometer comprises four drift chambers and a dipole magnet giving a horizontal transverse momentum kick of 0.265 GeV/c. The volume between drift chambers is filled with helium. The drift chambers consist of eight planes of sense wires, two horizontal, two vertical and two along each of 45° directions.

A quasi-homogeneous liquid krypton electromagnetic calorimeter with 127 cm (27 radiation length) long projective tower readout is used to measure photons from $\pi^0\pi^0$ events. The calorimeter has excellent resolution in energy (0.9% at average photon energy) and position (1.2 cm).

The summary of the basic features of the NA48 and KTeV detectors is given in Table 1. The numbers on NA48 performance are compiled from Ref. 6. The proper time resolution is calculated assuming average spatial resolutions along the beam direction (Z coordinate) and average kaon momentum.

One can see that both detectors have similar performance. For the two parameters used to reconstruct event kinematics, momentum/energy resolution and proper time resolution, the KTeV detector has a slight advantage. A better momentum resolution of the KTeV charged spectrometer is due to a larger field in the analysis magnet. Better resolution of the CsI calorimeter translates to a better proper time resolution for $\pi^0\pi^0$ events.

3 Data Analysis

The event reconstruction is similar for the both experiments, since the detector setups are very close. There are only small differences in the way some kinematic quantities are calculated. The main difference is in event tagging. KTeV uses the X position of the event vertex to determine the beam while NA48 relies on timing tagging to select the production target.

For the charged mode, tracks are reconstructed from the hits and drift times in the spectrometer. A vertex is defined as the point of closest approach of two oppositely charged tracks, provided they are separated by less than 3 cm in Z (NA48), or the χ^2 of the vertex fit is below 100 (KTeV). The experiments differ in the way the energy of the event is determined. NA48 ignores absolute track momentum information and reconstructs the energy using the opening angle between the tracks and the ratio of the track momenta, assuming the two tracks originate from $K \to \pi^+\pi^-$. KTeV uses a straight sum of the pion momenta. The NA48 method avoids systematic uncertainties

	KTeV	**NA48**
Beam Line		
Proton energy	800 GeV	450 GeV
Proton intensity per spill	$(2-8)\times 10^{12}$	1.1×10^{12}
Spill/Inactive time duration, sec	20/40	2.4/12.0
Kaon momentum range	$40-160$ GeV	$70-170$ GeV
Average kaon energy	70 GeV	110 GeV
Detector Setup		
Basic design	Double beam technique	
Source of K_S	Coherent regeneration	Secondary target
Event tagging	Vertex position	Timing tagging
Tracking		
Analysis Magnet P_t kick	0.412 GeV/c	0.256 GeV/c
Detector technology	Drift chambers	
Number of stations	2 before and 2 after magnet	
Planes per station	four, 2x2y	eight, 2x2y2u2v
Resolution per plane	100 μm	90 μm
Average per plane efficiency	99.5%	99.5%
Momentum resolution, σ_p/p	$0.2\%\oplus 0.008\%\times p$	$0.5\%\oplus 0.009\%\times p$
P resolution at P_{av}	0.4%	0.7%
Proper time resolution at P_{av}, $\Delta\tau/\tau_S$	6.1%	10.0%
Calorimetry		
Detector technology	CsI crystals	Liquid krypton
Spatial resolution	1.0 mm (small blocks) 1.8 mm (large blocks)	1.3 mm
Energy resolution, σ_E/E	$0.02/\sqrt{E}\oplus 0.005$	$0.125/E\ \oplus$ $0.032/\sqrt{E}\oplus 0.005$
Energy resolution at E_{av}	0.7%	0.9%
Proper time resolution at E_{av}, $\Delta\tau/\tau_S$	7.4%	8.5%

Table 1. Comparison of the basic parameters of NA48 and KTeV detectors

arising from the imperfect knowledge of the magnetic field flux, and pays the price of larger dependence on multiple scattering in the vacuum window. The magnetic field map is well known in the case of KTeV.

The semileptonic $Ke3$ background is rejected by requiring a low value of the ratio E/p of the energy of a matching cluster in the calorimeter to the track momentum. The cut is $E/p < 0.8$ (NA48) or $E/p < 0.85$ (KTeV). The $K \to \pi\mu\nu$ ($K\mu3$) background is rejected by requiring no hits in the muon veto detectors.

Good $\pi^+\pi^-$ events are selected by requiring the invariant mass of two pions to be close to the nominal kaon mass. This essentially eliminates differences between the methods used to reconstruct kaon momentum discussed above.

A further reduction of the background is achieved using a cut based on the kaon transverse momentum. NA48 defines p_t' which is the component of the kaon momentum orthogonal to the line joining the production target (K_L or K_S, identified by the Y vertex position) and the point where the kaon trajectory crosses the plane of the first drift chamber. The p_t' resolution is independent of the target from which the event originated. The distributions of p_t' for $\pi^+\pi^-$ events from different targets show similar shape.[6] NA48 selects events with $p_t'^2 < 2 \times 10^{-4}$ GeV^2/c^2.

KTeV has only one production target. For the good signal events, the kaon transverse momentum is equal to zero. The dominant source of large p_t^2 events in the Regenerator beam is due to diffractive scattering in the Regenerator. Therefore, p_t^2 is calculated assuming that the kaon scatters at the Z position of the downstream end of the Regenerator. After subtraction of the scattering background, the p_t^2 distributions in both beams are in fair agreement; some residual discrepancy is included in the systematic error. KTeV cuts at $p_t^2 < 2.5 \times 10^{-4}$ GeV^2/c^2. Simple calculations shows that this cut is actually much harder than the NA48 p_t' cut. Assuming the angles to be small, one can get

$$p_t^2 = p_t'^2 \times \left(\frac{L}{Z}\right)^2, \tag{7}$$

where L is the distance from the target to the NA48 first drift chamber (about 210 m and 90 m for K_L and K_S target, respectively) and Z is the distance from the target to the decay vertex. For a K_L event decaying in the middle of the decay region, $Z = 140$ m, one gets $p_t^2 = 2.25 \times p_t'^2$. The difference between transverse momentum definitions becomes even larger for K_S events.

The neutral mode reconstruction starts with identifying four clusters in the electormagnetic calorimeter with energies above 3 GeV. The clusters are required to have photon-like shape and to be in time. Fiducial cuts are applied to ensure the photons are well measured. The minimum distance between photon candidates is required to be greater than 10 cm (NA48) or 7.5 cm (KTeV). The $K_L \to 3\pi^0$ background is reduced by requiring no extra clusters of energy above about 1.5 GeV.

The kaon energy is obtained from the sum of photon energies. To determine the longitudinal position of the decay vertex relative to the front of the calorimeter, NA48 uses the energies and positions of the four selected clusters and assumes that their invariant mass is the kaon mass. Next, three possible combinations of photon clusters into π^0 pairs are tried; the event is selected if one of the combinations has acceptable quality.

KTeV chooses an alternative method. First, all three pairings of photons into π^0 candidates are tried. For each π^0 candidate, the Z vertex is reconstructed using energies and positions of the photons and assuming that their invariant mass is the pion mass. The pairing with the best agreement of the two π^0 vertices is chosen; the event is rejected if the best pairing has a poor quality. The vertex of the kaon decay is determined as a weighted average of the two π^0 vertices. Finally, the invariant mass of the four photon clusters is reconstructed; it is required to be close to the nominal mass of the kaon.

The X and Y position of the decay vertex is determined using the line connecting the production target and the center of energy of the photon clusters. For NA48, the production target is defined by the timing tagging. For KTeV, the X position of the vertex is used to define the beam. KTeV requires that X and Y positions of the vertex are within one of the two beams. Since the separation between the beams is larger than the transverse position resolution (10 cm compared to 1 mm), the X-position tagging always gives the correct beam for a signal, non-scattered event. For events scattered in the Regenerator, there is a certain probability to leave the Regenerator beam and decay in the range of Vacuum beam, contributing as a *cross over* background.

KTeV uses $\pi^+\pi^-$ events, for which complete reconstruction of the kinematics is possible, to study regenerator scattering background. The scattering background consists of an inelastic and a diffractive part. Empirically, the former has a relatively flat p_t^2 spectrum and can be described as a pure K_S state. The latter can be further subdivided into single, double and multiple scattering off Carbon, scattering off Lead and scattering off Hydrogen. Each of the terms has its own p_t^2 dependence and can be represented as a coherent mixture of K_S and K_L states. Other small backgrounds include diffractive dissociation reactions $n + C_{12} \to C_{12} + K_S\Lambda$ and $K_L + C_{12} \to C_{12} + K_S\phi$,

$\phi \to K_S K_L$ with non-reconstructed Λ or one K_S particle missing, as well as Primakoff K^* production: $K_L + Pb \to Pb + K_S^*$, $K_S^* \to K_S + \pi^0$ with missing π^0.

The scattering background is parametrized and put into the Monte Carlo simulation. This simulation is tuned to fit the charged mode data. The same Monte Carlo model is used to predict background shapes for $\pi^0\pi^0$ events. The regenerator scattering background for $K_S \to \pi^0\pi^0$ events is estimated to be about 1%. The contribution of the cross over background for $K_L \to \pi^0\pi^0$ events is about 0.3%. The systematic uncertainty in $\mathrm{Re}(\epsilon'/\epsilon)$ from the background subtraction is about 0.7×10^{-4}. This number includes uncertainties in the charged mode p_t^2 acceptance as well as possible difference in the inelastic background levels between charged and neutral modes because of residual differences in the veto cuts.

The timing tagging is a unique feature of the NA48 experiment.[6] The event is tagged by classifying it as K_S if there is a proton within a ± 2 ns coincidence window centered on the event time; otherwise the event is classified as K_L.

An accidental coincidence between a proton traversing the tagger and a K_L event may cause the event to be wrongly counted as K_S. This probability is measured for $\pi^+\pi^-$ events, using the Y position of the vertex as an alternative tagging technique, to be $\alpha_{LS}^{+-} = (11.05 \pm 0.01)\%$ (1998 data[7]). The measurement of the double ratio is sensitive to the difference in this probability between $\pi^0\pi^0$ and $\pi^+\pi^-$ events. The latter was estimated by various techniques to be $(0.3 \pm 4.2) \times 10^{-4}$.

4 Results

Table 2 summarizes event yields collected by the experiments. So far we have three reported measurements of $\mathrm{Re}(\epsilon'/\epsilon)$: the first published KTeV result based on the 1996 $\pi^0\pi^0$ data and the $\pi^+\pi^-$ data collected in the first quarter of 1997 (**KTeV 96-97a**); the first published NA48 result based on the 1997 data (**NA48 97**) and a preliminary result announced by NA48 based on the data collected in 1998 (**NA48 98**). The last row in Table 2 (**KTeV 97-97b**) shows yields for the KTeV data collected in 1997 (complete 1997 for $\pi^0\pi^0$ events and last three quarters of 1997 for $\pi^+\pi^-$ events). The analysis of this sample is not yet finished.

The next step from event yields is to calculate $\mathrm{Re}(\epsilon'/\epsilon)$ according to formula (6). An obvious problem arises, however. As the K_L and K_S lifetimes are very different, so are the decay Z distributions and thus the event yields, integrated over the large Z range, are different as well. Furthermore, the detector acceptance is not constant in Z;

	$N(K_L \to \pi^+\pi^-)$ $\times 10^6$ events	$N(K_S \to \pi^+\pi^-)$ $\times 10^6$ events	$N(K_L \to \pi^0\pi^0)$ $\times 10^6$ events	$N(K_S \to \pi^0\pi^0)$ $\times 10^6$ events
KTeV 96-97a[5]	2.6	4.5	0.9	1.4
NA48 97[6]	1.1	2.1	0.5	1.0
NA48 98[7]	4.8	7.5	1.1	1.8
KTeV 97-97b	7.1	12.3	2.5	4.2

Table 2. Data sets and event yields. The **KTeV 96-97a** data sample comprises $\pi^0\pi^0$ data collected in 1996 and $\pi^+\pi^-$ data collected in the first quarter of the 1997 running period ("97a"). The **KTeV 97-97b** sample consists of $\pi^0\pi^0$ data collected in the 1997 running period and $\pi^+\pi^-$ data collected in the last three quarters of 1997. The **NA48 97** and **NA48 98** data samples are based on the 1997 and 1998 running periods, respectively.

it is also unequal for $\pi^+\pi^-$ and $\pi^0\pi^0$ events.

The collaborations took alternative paths to resolve this problem. NA48 uses a technique of *weighting* K_L events according to their proper decay time, so that the effective longitudinal vertex distribution of K_L events is made equal to the K_S distribution. The residual acceptance differences, mainly due to difference in production targets and beam divergences, are studied with a full simulation of the beams and detector.

KTeV relies on detailed Monte Carlo simulation to determine the detector acceptance. The collaboration uses the weighting method as a cross check.

Both methods have advantages and disadvantages. An obvious disadvantage of the weighting technique is the increase in statistical uncertainty, since the K_L events reconstructed far from the K_S production target are effectively not counted. An obvious disadvantage of the Monte Carlo correction is an additional systematic uncertainty coming from determination of the detector acceptance in Z.

The quality of the Monte Carlo simulation can be checked by its ability to reproduce the data Z distribution in the Vacuum beam. This can be studied for the signal $\pi^+\pi^-$, $\pi^0\pi^0$ as well as for the high statistics $Ke3$ and $3\pi^0$ events. Figure 3 shows Z distributions of $\pi^+\pi^-$ and $Ke3$ events for KTeV data collected in the last three quarters of 1997 running period ("97b"), compared to the Monte Carlo simulation. A linear slope in the straight line fit to the ratio of the data to the Monte Carlo distributions is a direct measure of the bias in $\mathrm{Re}(\epsilon'/\epsilon)$. Since the average Z position in the Vacuum beam differs by about 6 meters in Z relative to the Regenerator beam, a slope of 1×10^{-4} m^{-1} corresponds to about a 1×10^{-4} shift in $\mathrm{Re}(\epsilon'/\epsilon)$. The 97b data show that the slope is

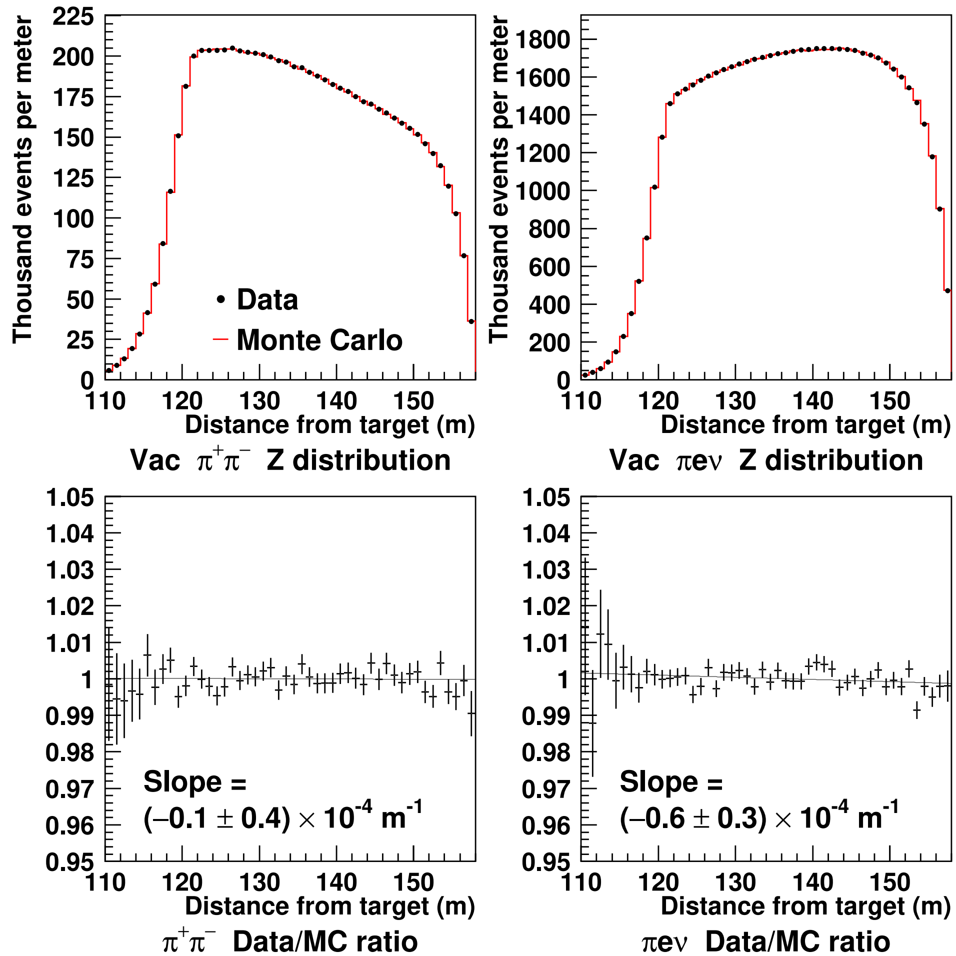

Fig. 3. Distribution of decay vertex position for $K \to \pi^+\pi^-$ events (upper left plot) and for $K \to \pi e \nu$ events (upper right plot). The KTeV $1997b$ data are shown as points with error bars; the histogram represents Monte Carlo simulation. The two bottom plots show the ratio of data to Monte Carlo distributions.

consistent with zero. This was not the case for the data collected in the first quarter of 1997 ("97a") which was used for the first KTeV result on $\mathrm{Re}(\epsilon'/\epsilon)$.[5] In fact, this slope was the dominant source of the systematic uncertainty in the result.

Table 3 gives a summary of systematic uncertainties of the $\mathrm{Re}(\epsilon'/\epsilon)$ measurements. The numbers are combined into groups for an easier comparison between experiments. "Trigger efficiency" includes losses of $\pi^+\pi^-$ and $\pi^0\pi^0$ events during data taking. For KTeV, the largest contribution is from the level 3 software filter. For NA48, it is dominated by level 1 losses of $\pi^+\pi^-$ events.

"$\pi^+\pi^-$ reconstruction" comprises uncertainties arising from the knowledge of the momentum scale, from the detector alignment and calibration and from the analysis cut variation. "$\pi^0\pi^0$ reconstruction" covers calorimeter energy scale and linearity, alignment and cut variation. The key source for the charged mode is the analysis cut variation. For the neutral mode, knowledge of the energy scale and linearity are the most important.

"Acceptance", in the case of KTeV, includes all uncertainties in Monte Carlo simulation: description of the limiting apertures, of the detector resolution, modeling of the drift chamber efficiency. This item also includes overall checks based on the Z-slope in the Vacuum beam; the slope in the charged mode is the dominant source of this uncertainty ($\Delta(\mathrm{Re}(\epsilon'/\epsilon)) = 1.6 \times 10^{-4}$). For NA48, "Acceptance" includes uncertainties in residual differences between K_S and K_L beams, as well as a small contribution from scattering off detector elements.

"Background" includes backgrounds in charged and neutral decay modes. For KTeV, the largest contribution comes from uncertainties in modeling the regenerator scattering background.

"Event tagging" and "Accidental effects" are the sources specific to the NA48 experiment. KTeV is practically insensitive to the biases coming from accidental activity since it uses identical beams for K_L and K_S events. Any extra detector activity is essentially the same for events from Vacuum and Regenerator beam. Residual effects are included in the uncertainty of the drift chamber simulation and the calorimeter energy scale. The situation is different for NA48 since the K_L and K_S beams are very different.

"Regenerator parameters" is the source specific for KTeV. It includes uncertainties in measuring of transmission and regeneration, as well as uncertainties of the external parameters, τ_S and Δm.

The values for the direct CP violating parameter $\mathrm{Re}(\epsilon'/\epsilon)$ measured by KTeV and

	KTeV 96-97a $\times 10^{-4}$	NA48 97 $\times 10^{-4}$	NA48 98 $\times 10^{-4}$
Trigger efficiency	0.6	3.8	1.8
$\pi^+\pi^-$ reconstruction	0.5	0.8	0.3
$\pi^0\pi^0$ reconstruction	1.3	2.0	1.7
Acceptance	2.0	2.1	1.6
Background	0.8	0.7	0.6
Event tagging	–	1.8	1.4
Accidental effects	–	2.3	2.0
Regenerator parameters	0.3	–	–
Total	2.8	5.7	4.0

Table 3. Sources of systematic uncertainty of the $\mathrm{Re}(\epsilon'/\epsilon)$ measurements. The numbers are combined in groups according to the procedure given in the text (see Section 4) for easier comparison between the experiments. The "Total" line shows the total systematic uncertainty given by each experiment.

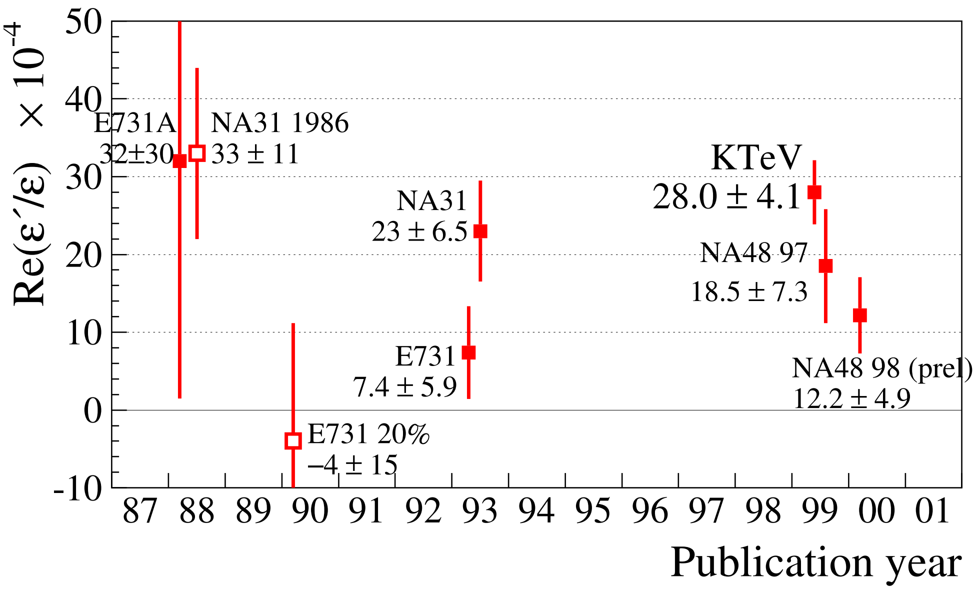

Fig. 4. Recent measurements of $\mathrm{Re}(\epsilon'/\epsilon)$. Open squares show measurements based on subsets of data samples superseded by the subsequent publications.

NA48 are:

KTeV 96-97a:[5]	$(28.0 \pm 3.0\,(stat) \pm 2.8\,(syst)) \times 10^{-4}$	$=$	$(28.0 \pm 4.1) \times 10^{-4}$,
NA48 97:[6]	$(18.5 \pm 4.5\,(stat) \pm 5.8\,(syst)) \times 10^{-4}$	$=$	$(18.5 \pm 7.3) \times 10^{-4,}$
NA48 98:[7]	$(12.2 \pm 2.9\,(stat) \pm 4.0\,(syst)) \times 10^{-4}$	$=$	$(12.2 \pm 4.9) \times 10^{-4}$

NA48 also quotes the combination of their published[6] and preliminary[7] results:

$$\mathrm{Re}(\epsilon'/\epsilon) = (14.0 \pm 4.3) \times 10^{-4} \quad \textbf{NA48 97-98, combined.}$$

Figure 4 shows all world measurements of $\mathrm{Re}(\epsilon'/\epsilon)$. Assuming that systematic errors are uncorrelated between experiments and different experimental results are consistent with each other, we obtain the following value for $\mathrm{Re}(\epsilon'/\epsilon)$:

$$\mathrm{Re}(\epsilon'/\epsilon) = (19.3 \pm 2.4) \times 10^{-4}\ (5\% c.l.) \quad \textbf{World Average}$$

This result definitively establishes the existence of direct CP violation and thus confirms the prediction of the Standard Model. It also shows that a Superweak interaction cannot be the sole source of CP violation in the neutral kaon system.

Further experimental results from both collaborations will be available soon. KTeV is close to completing the analysis of the 1997 data which more than doubles the sample used for the first publication. Another factor of two in statistics will come from the 1999 data. NA48 plans to reduce the systematic uncertainty in $\mathrm{Re}(\epsilon'/\epsilon)$ for the 1998 data sample before publishing the analysis. The detector continues data-taking and analysis of the 1999 data is on the way. The statistical uncertainty of $\mathrm{Re}(\epsilon'/\epsilon)$, combining the data from both collaborations, is expected to be lower than 1×10^{-4}.

After the first exciting news about the existence of direct CP violation the measurement of $\mathrm{Re}(\epsilon'/\epsilon)$ enters the phase of establishing the exact value of this important parameter. Careful detector design, large data samples and assiduous data analysis make this possible.

References

[1] J.H Christenson, J.W. Cronin, V.L. Fitch, and R. Turlay, Phys. Rev. Lett. **13**, 138 (1964).

[2] Particle Data Group, C. Caso *et al.* Eur. Phys. J. C**3**, 1 (1998).

[3] W. Ochs, πN Newsletter **3**, 25 (1991).

[4] L. Wolfenstein, Phys. Rev. Lett., **13**, 562 (1964).

[5] A. Alavi-Harati *et al.*, Phys. Rev. Lett. **83**, 917 (1999).

[6] G. Anzivino *et al.*, Phys. Lett. **B 465**, 335 (1999).

[7] R.G. Cassagnac, Proceedings Rencontres de la vallee d'Aoste, la Thuile (2000).